Springer

KSME

Journal of Mechanical Science and Technology 26 (1) (2012) 223~233
www.springerlink.com/content/1738-494x
DOI 10.1007/s12206-011-0801-5

Optical investigation of the fuel injector influence in a PFI spark ignition engine for two-wheel vehicles †

Simona Silvia Merola*, Cinzia Tornatore and Paolo Sementa

Istituto Motori, via G. Marconi 8, 80125 Napoli, Italy

(Manuscript Received March 20, 2010; Revised July 11, 2011; Accepted July 26, 2011)

Abstract

This paper describes the results obtained in a port fuel injection spark-ignition (PFI SI) engine by optical diagnostics during the fuel injection and the combustion process. A research optical engine was equipped with the fuel injection system, the head and the exhaust device of a commercial 250 cc engine for scooters and small motorcycles. Two injectors were tested: standard 3-hole injector that equipped the real reference engine and a 12-hole injector. The intake manifold was modified to allow the visualization of the fuel injection using an endoscopic system coupled with CCD camera. Size and number of the fuel droplets were evaluated through an image processing procedure. The cycle resolved visualization and chemiluminescence allowed to follow the combustion process from the spark ignition to the exhaust phase. All the optical data were correlated with engine parameters and exhaust emissions. The effect of the fuel injector type on deposits formed by fuel accumulation and dripping on the intake valves steams and seats was investigated. In particular, the evolution of diffusion-controlled flames due to the fuel deposits burning was analyzed. These flames were principally located near the intake valves, and they persisted well after the normal combustion event. The consequences were the formation and emission of soot and unburned hydrocarbons. The multi-hole injector helped reducing wall wetting and deposit formation so that the emission characteristic can be improved. The use of 12-hole injector allowed a more homogeneous distribution for a lower time of fuel droplets in the intake manifold than the 3-hole injector. This study also investigated the detailed physical/chemical phenomena to figure out reasons for the improvement using optical measurements.

Keywords: Spark-ignition engine; Gasoline; Optical diagnostics; Fuel injector; Two-wheel vehicle; Combustion process

1. Introduction

In recent years the need to meet ever more stringent emission regulations and to increase fuel economy has led to significant development of gasoline spark ignition combustion engines. In the field of automotive engines, many topics have been investigated, ranging from in-cylinder flow to mixture formation and flame propagation structure [1, 2]. Processes in port fuel injection spark-ignition (PFI SI) engines now are reasonably well understood thanks to synergy between the traditional combustion-heat-release analysis, emissions measurements, and quasi-dimensional modeling with the optical diagnostics and CFD analysis.

On the other hand, little work has been done in this area for two-wheel vehicle engines, in particular for small-motorcycle and scooter engines. One of the difficulties is that the scooters and motorcycles vary considerably depending on the task for which they are designed, such as long distance travel, navigating congested urban traffic, cruising, sport and racing, or off-road conditions. Moreover they are the most affordable form of motorized transport; in some parts of the world they are also the most widespread transport.

Around the world, emission regulations for two-wheel vehicles are different; nevertheless, the standards are becoming ever more severe. The Euro III regulations impose strong reduction in NOx, HC and CO emission. On the other hand, the market requirements range from high-performance of recreational bikes to the economy-oriented basic transportation. A major challenge for combustion scientists and engine-development engineers is to optimize engine combustion to improve fuel economy, lower pollutant emissions while maintaining outstanding performance, durability, and reliability at an affordable price. To this purpose, the fundamental research plays a significant role and optical techniques represent a powerful tool. There are various methods that can be used to study spray and combustion within an optically accessible engine. Different methods provide different information. Using visualization methods, macroscopic parameters can be determined, and using the PIV [3], LIF and PDPA techniques, information can be found regarding the microscopic parame-

† This paper was recommended for publication in revised form by Associate Editor Kyoung Doug Min

* Corresponding author. Tel.: +39 081 7177224
E-mail address: s.merola@im.cnr.it

ters. However, for combustion characteristics studies, visualization technique is very useful in gathering information from the combustion chamber.

Already in the first part of 1900, high-speed film imaging combined with combustion heat-release analysis [4] proved that engine combustion occurred as a wrinkled premixed turbulent flame-front with considerable cycle-to cycle variability. High-speed photography of in-cylinder flows and fuel sprays in a motored transparent liner engine, and high-speed Schlieren movies of combustion in a firing engine provided insight into in-cylinder processes in spark-ignition gasoline aircraft engines [2].

Work has been conducted in either modified engines or constant-volume vessels, with both systems being equipped with an optical access made of quartz or fused silica. More investigations have to be carried out on the fundamentals of spray and combustion of fuel in IC engines [5, 6].

Optical diagnostics applied to PFI SI engines allowed to identify one of the most important phenomena that takes place in this kind of engine: the wall-wetting and fuel film formation. In PFI SI engines, the atomized fuel is sprayed towards the intake valves, where it may evaporate, puddle or rebound [7-9]. A portion of fuel may flow directly into the cylinder or impinge upon the port walls. These phenomena occur in varying degrees and depend upon the engine design, injector location and engine operation. Potentially, the fuel can enter the cylinder in a poorly atomized state, leading to increased unburned hydrocarbon emissions. This is particularly true during cold operation, when evaporation is low. In the small-motorcycle and scooter engines fuel injection occurs in intake manifolds smaller than light-duty vehicle engines, increasing the criticism of fuel-wall interaction. At the moment, a simultaneous study of in-cylinder mixture formation, combustion process and exhaust emission has never been performed in such a small SI engine. In particular, there is no information in the scientific literature about the influence of the port fuel injector on the phenomena that take place in a small engine for motorcycles. In the present study two commercial multi-hole injectors were tested. Experimental investigations were performed in a single cylinder engine constituted by an elongated optical accessible piston and equipped with the head and injection system of a reference 4-stroke engine for 2-wheel vehicle. High spatial resolution imaging was applied to analyze the fuel injection phase. The cycle resolved visualization was used to follow the flame propagation from the spark ignition to the exhaust phase. Chemiluminescence measurements were realized to follow the CH radicals distribution in the combustion chamber.

The experiments described in the paper are part of the research activities realized in order to optimize 4-stroke engines for 2-wheel vehicles with low cost solutions. An understanding of the thermal and chemical phenomena connected to the improvement of the mixture formation and to the wall-wetting and fuel deposits reduction allows one to evaluate costs/benefits due the change of injector and to fix the industrial strategies. In general, the optical diagnostics can be useful in the future for the new generation engines for small urban vehicles too. In fact, these basic experiments can furnish important data for the optimization of the whole engine design and for the calibration of 1D-3D simulations and numerical methodologies in order to reduce the costs and to avoid the anachronistic try-and-error method.

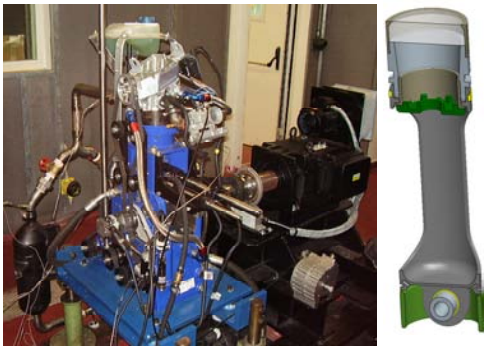

Fig. 1. Photograph of the engine and sketch of the elongated optically accessible piston.

2. Experimental apparatus

2.1 Optically accessible engine

The experimental investigations were performed on an optically accessible single-cylinder, PFI, four-stroke SI engine. The engine bore and stroke were 72 mm and 60 mm, respectively, and the geometric compression ratio was 11. The engine was equipped with the cylinder head of a commercial 250 cc engine for scooters and small motorcycles. A four-valve, pent-roof chamber engine was mounted on an elongated piston. The engine reached a maximum speed of 5000 rpm, where the maximum performance is 7.9 kW and 14.7 Nm. These values are calculated considering a mechanical theoretical efficiency of 85%, since the real efficiency of experimental engines is lower than real engines because of higher friction losses. The head had a centrally located spark plug and a quartz pressure transducer was flush-installed in the combustion chamber to measure the combustion pressure. The in-cylinder pressure, the rate of chemical energy release and the related parameters were evaluated on an individual cycle basis and/or averaged on several consecutive cycles [10]. A lambda sensor was installed at the engine exhaust for the measurement of the air/fuel ratio. A photograph of the engine with a sketch of the elongated optically accessible piston is reported in Fig. 1.

Two commercial injectors with 3 holes and 12 holes were tested. The first one was the standard injector for the real reference engine; the second one was selected among the commercial injectors more well-matched with the intake manifold and experimental operating condition. The Sauter mean diameter was 96 μm and 65 μm for 3-hole injector and 12-hole one, respectively. The positions of the holes on the injector tip are shown in Fig. 2.

Fig. 2. The spatial distribution of the holes on the two tested injectors.

A special customized lube oil and coolant conditioning unit for transparent single cylinder engine application was used. The conditioning unit contains two pumps: one for oil and one for water. The oil pressure in the circuit can be adjusted through a pressure control valve (spill valve). A coolant heater, installed in the cooling water circuit, was foreseen to heat up engine coolant during engine operation as well as engine lube oil via the coolant/oil heat exchanger.

A section of the flat-bottomed piston was replaced with an optical piston with a gasket ring to mount a flat sapphire window to enable the passage of optical signals coming from the combustion chamber. To reduce the window contamination by lubricating oil, the elongated piston arrangement was used together with self-lubricating Teflon-bronze composite piston rings in the optical section.

2.2 Setup for optical measurements

The fuel injection was visualized using an endoscopic system coupled with a 12-bit CCD color camera equipped with a 50 mm focal length, F/3.8 Nikon lens. The CCD had a 640 x 480 pixel matrix with a pixel size of 9.9 x 9.9 μm^2. This optical assessment allowed a spatial resolution around 90 µm/pixel. The spectral range of the camera was 290-800 nm. The exposure time was fixed at 55.5 µs, which corresponds to 1 CAD at an engine speed of 3000 rpm. The dwell time between two consecutive images was set at 55.5 µs. The fuel spray was illuminated by flash cold pulsed light source through an optical fiber. A sketch of the optical set-up for the fuel injection visualization is reported in Fig. 3a. The CCD was not a cycle resolved detector; each acquisition was performed at a fixed crank angle of different engine cycles. The endoscopic system (rigid boroscope and light guide) was flush-installed in the intake manifold wall in order to maintain unchanged the fluid-dynamic condition in the manifold.

The combustion process was investigated using the experimental apparatus shown in Fig. 3b. The radiations emitted passed through the sapphire window and they were reflected toward the optical detection assembly by a 45° inclined UV-visible mirror located at the bottom of the engine.

Cycle resolved flame visualization was performed by 8-bit high speed camera (512 x 512 pixel) equipped with a 50 mm focal Nikon lens. The spectral range of the high speed camera

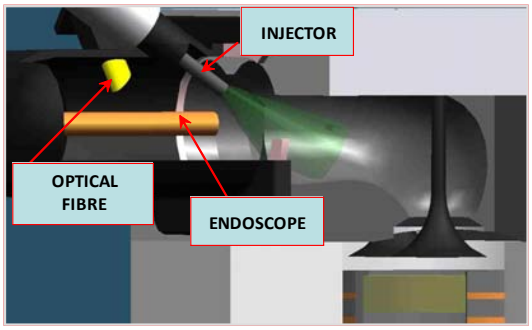

(a)

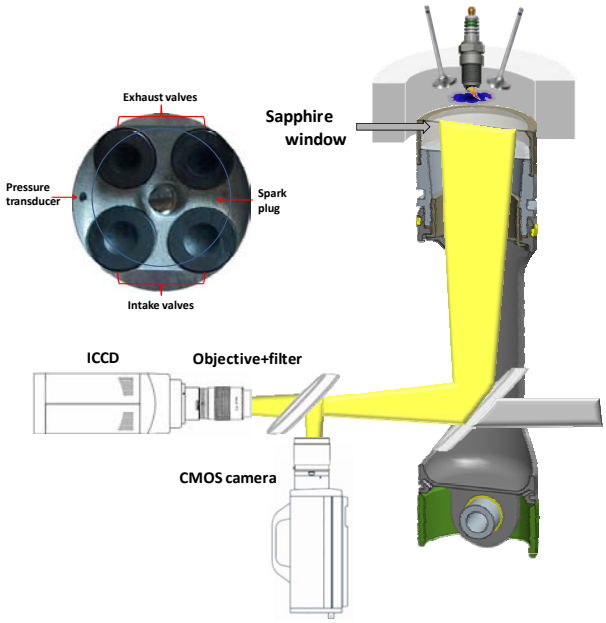

(b)

Fig. 3. Sketch of the experimental setup for the optical investigations: (a) in the intake manifold; (b) in the combustion chamber.

extended from 400 nm to 900 nm. A camera region of interest was selected (360 x 360 pixel) to obtain the best match between spatial and temporal resolution. This optical assessment allowed a spatial resolution around 0.25 mm/pixel and a frame rate of 7188 fps. The exposure time was fixed at 10 µs. AVL Indimodul recorded the TTL signal from the camera acquisitions together with the signal acquired by the pressure transducer. It was possible to determine the crank angles where optical data were detected.

CH chemiluminescence measurements were performed by an ICCD equipped with an F/3.8 UV Nikon objective with 78mm focal length. The ICCD had an array size of 512 x 512 pixels with a pixel size of 19 x 19 μm^2 and 16-bit dynamic range digitization at 100 kHz. The ICCD spectral range spread from UV (180 nm) until IR (900 nm). A band-pass filter centered at 430 nm with 5 nm half height width was used to detect CH radical emission. The spatial resolution was around 0.12 mm. To enhance the signal noise ratio, five acquisitions for each crank angle were carried out. Exposure time and

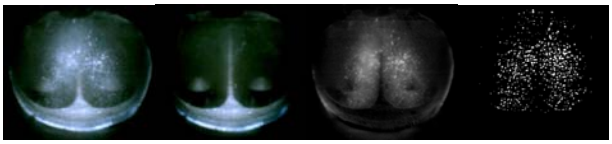

(a) (b) (c) (d)

Fig. 4. Sketch of the image processing for the retrieving of the fuel injection optical data.

(a) (b) (c) (d)

Fig. 5. Sketch of the image processing for the retrieving of the combustion process optical data.

dwell time between two consecutive images were set at 55.5 μs.

The crank angle encoder signal synchronized all the cameras and the engine through a unit delay device.

Post-detection image processing was realized to retrieve the optical data detected during the fuel injection and during the combustion process. For both the phases, our aim was not to propose new methodologies, but only to compare the results obtained using the two tested injectors. The potential biases in the applied methodology for the digital image processing had the same weight in a relative balance of the experimental results due to the two injectors. All the computations needed for the processing of the images have been done using National Instruments programs (Vision Assistant and LabView).

About the fuel injection visualization, the fundamental steps of the image processing are reported in Fig. 4. In the imaging set-up the objects under consideration are droplets of liquid illuminated by a white, non-coherent light source. The first step consisted in the subtracting from the selected image (a) of the background (b). Then the resulting color image was changed in gray-scale image by the extraction of the luminance plane (c). To characterize the droplets, each droplet should be individually localized on the pictures. This is usually done by a classic threshold applied to the picture at a given level. This is the correct approach if all the droplet images to be analyzed have the same contrast. Instead, the smallest or most unfocused droplets have a low contrast and can be lost by the threshold methodology. To increase the sensitivity of the detection, a two-step convolution filter was applied before the threshold analysis. This filter highlights (by squared function) the pixels that have the edges (peak and valley) firstly in a kernel size equal to 7 x 7 and then equal to 3 x 3 [11, 12]. After convolution the threshold filter based on interclass variance was applied (d). The droplet radius is based on the area size, considering the circular shape. To calibrate the sizing procedure, a reticule with 100 x 100 μm cells was placed in the engine intake manifold. The reticule was visualized with the same optical setup used for the fuel injection imaging. The reticule was translated in the manifold by 100 steps. The variation due to the lateral magnification resulted negligible. The procedure was limited by the spatial resolution of the optical setup. It fixed at 90 μm the cut-off diameter.

Post-detection image processing for the analysis of combustion process was applied too. As schematically reported in Fig. 5, the region of interest retailed from 8-bit image (a) was converted in a binary-scale image by the threshold filtering based on clustering statistical technique (b). Then small and border objects were removed by 3 x 3 erosions (c). Finally, the interior contour was extracted (d). The image analysis allowed us to evaluate area, perimeter, maximum Feret diameter and equivalent ellipse axis. In this work the mean radius was calculated by average between ellipse axis.

Moreover, each 8-bit cycle-resolved image was converted in a numerical matrix. In this way it was possible to evaluate the integral luminous signal and the local signal related to each point of the combustion chamber [13, 14].

2.3 Exhaust measurements

Steady-state measurements of CO, CO2, HC and NOx were performed in the undiluted exhaust. Gaseous emissions were measured by AVL Digas 4000 constituted by an electrochemical sensor for NOx and non-dispersive infrared (NDIR) analyzers for HC, CO and CO2. Smoke was measured by a part flow smoke opacimeter (AVL Opacimeter 439). The opacity can be directly correlated to the particulate mass concentration [15].

3. Results and discussion

All the experimental investigations were carried out at an engine speed of 3000 rpm at wide open throttle. The intake air temperature was fixed at 298 K and the cooling water temperature was set at 333 K. Euro 4 gasoline was injected at 3 bar. The end of fuel injection occurred at 60 CAD ATDC, and the injection durations were fixed in order to reach the stoichiometric equivalence ratio (Φ=1.0 ± 1%). The lambda value was measured by an oxygen sensor at the engine exhaust. The valve-timing diagram is reported in Fig. 6. For all the test cases, the electronic spark timing was fixed to operate at the maximum brake torque. The details of engine performance at the selected operating conditions are reported in Table 1. The engine power, IMEP and COV were good as the commercial reference engine. This demonstrated that the thermal evolution due to the heat transfer among the different components of the optical engine could be considered as satisfactorily negligible. It should be noted that the IMEP values can be considered comparable. Thus the conventional and preliminary analysis shows a decrease in the fuel specific consumption for the 12-hole case with respect to 3-hole.

Pressure measurements and exhaust data give real-time cycle-resolved overall information on the combustion process

Table 1. Details of the selected engine operating conditions.

	DOI [CAD]	IMEP [bar]	COV_{IMEP} [%]
3-hole	175	6.78	0.9
12-hole	135	6.86	0.8

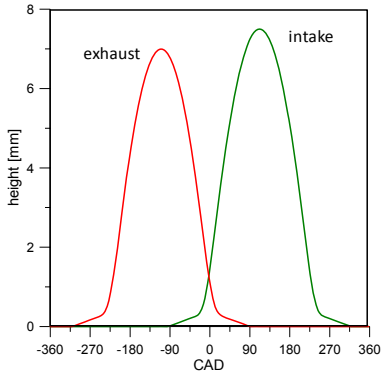

Fig. 6. Engine valve-timing diagram.

but they don't allow local investigations. Optical techniques are a powerful tool for detailing thermal and fluid dynamic phenomena that occur in the intake manifold and in the combustion chamber. On the other hand, these methodologies need high-cost specific engines and instrumentations. In this work, high spatial resolution visualization of injection phase and combustion process was performed.

Fig. 7 reports a selection of images detected during the fuel injection phase. The first droplets for the 3-hole injector were detected at 60 CAD BTDC instead of 115 CAD BTDC; this was due to the delay induced by the inertia of the injection system in relation to the electronic injection signal. The fuel droplets resulted well optically resolved; thus, their mean diameter was bigger than CCD spatial resolution. The injector sprayed the fuel towards the plate between the intake valves and on the intake valves steams. The droplets impingement induced fuel deposits formation on the intake manifold walls. The fuel deposits were drawn by gravity on the valve head where they remained as film due to the surface tension [6, 16].

At TDC, the intake valves lift is around 1 mm. From this point, a part of the droplets was carried directly into the combustion chamber by the gas flow. This effect is well observable since 30 CAD ATDC. The droplets were sucked in the combustion chamber and then they stuck on the cylinder walls and on the piston surface. The first evidence of fuel droplets for the 12-hole injector was detected around 30 CAD BTDC instead of 75 CAD BTDC: the delay time for the effective injection resulted shorter than 3-hole injector. Also in this case, the fuel injection occurred partly before and partly after the intake valves opening. The amount of fuel injected when the intake valves were closed is lower than the 3-hole injector. As a consequence, the impingement on the intake valves was reduced and the fuel film deposition as well. The image processing previously described allowed us to evaluate the number

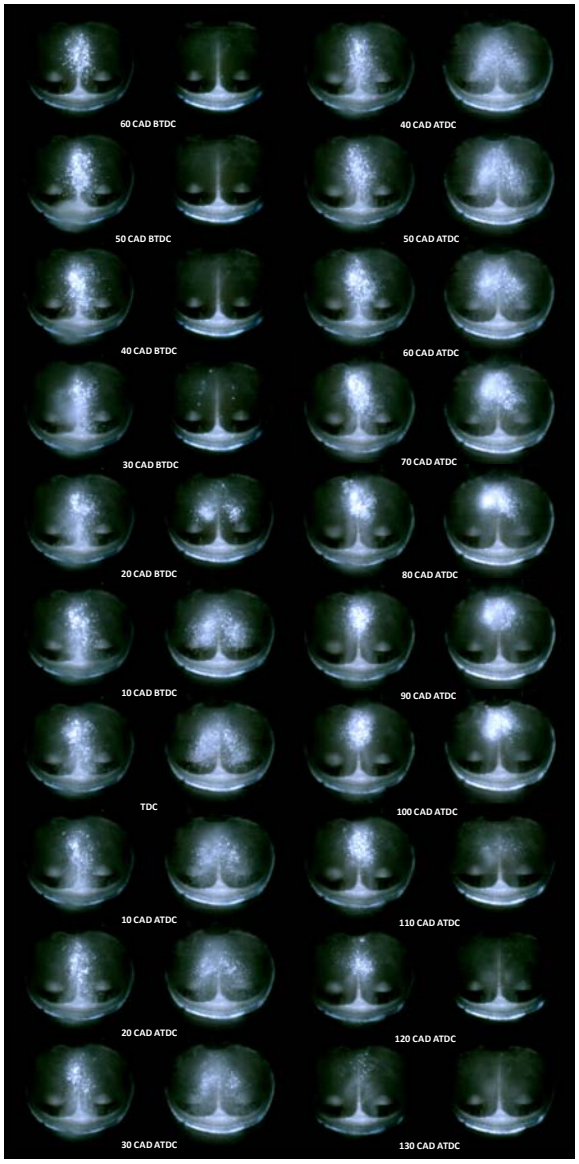

Fig. 7. Images detected in the intake manifold during the fuel injection phase.

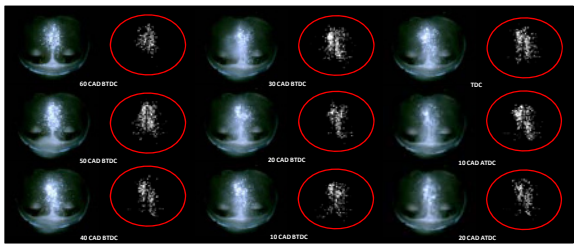

Fig. 8. Comparison between the raw image (left) and processed image (right) for the 3-hole injector.

density of the droplets in the intake manifold. Fig. 8 shows the effect of the image processing on the raw optical data for an image selection related to the 3-hole injector.

Fig. 9 shows the number density versus the droplet radius

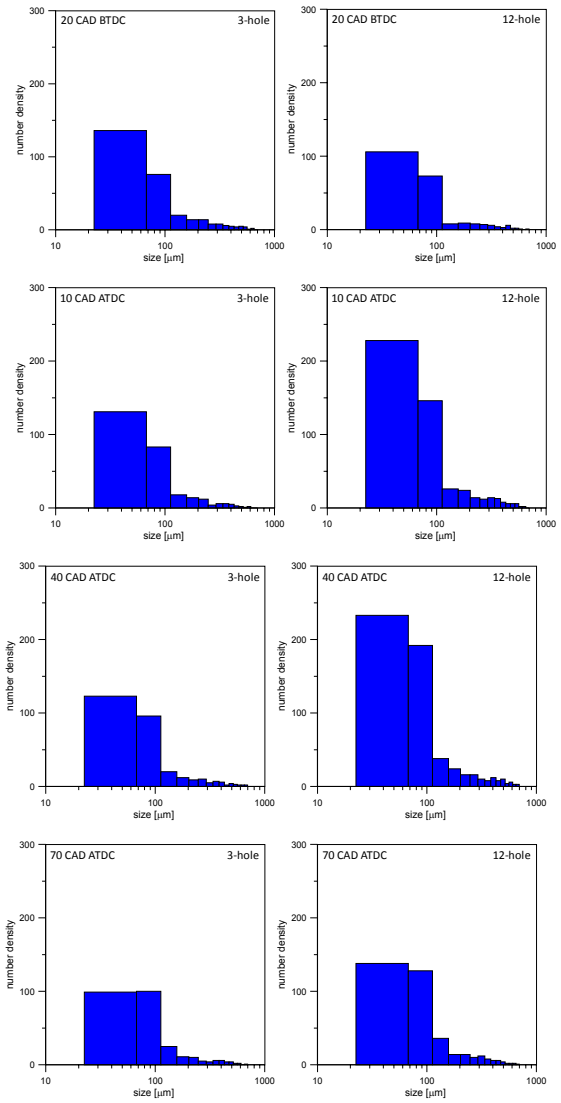

Fig. 9. Droplet size distribution evaluated by fuel injection visualization.

evaluated at selected crank angles. At 20 CAD BTDC, the intake valves can be considered as closed (valve lift <0.5 mm). The fuel injection occurred more than 40 CAD for the 3-hole injector and from more than 10 CAD for the 12-hole injector. As a consequence of the low turbulence level, the total droplet numbers were approximately equivalent. A higher number of small droplets was evaluated for the 3-hole injector than the 12-hole due to the different injection timing. At 10 CAD ATDC, the intake valve lifts were around 30% and the flow field towards the combustion chamber was low. The droplets mean size became bigger for the 3-hole injector than 12-hole due to a stronger coalescence process. The number of small droplets increased for the 12-hole injector. At 40 CAD ATDC, the intake valves opened around 65% and the gas flow increased the turbulence in the intake manifold near the intake valve gap. This induced an enhancement of the coalescence with respect to the simultaneous concurrent evaporation effect

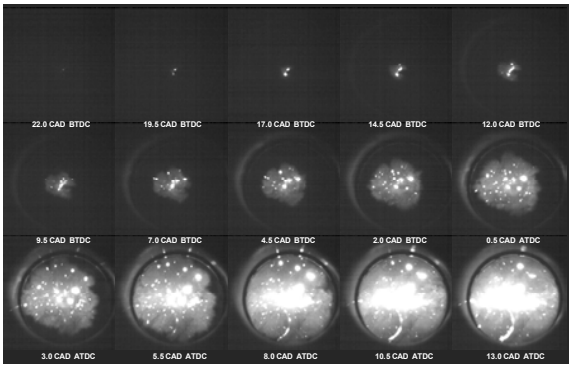

Fig. 10. Images detected in the first phase of the combustion process for 3-hole injector (single cycle).

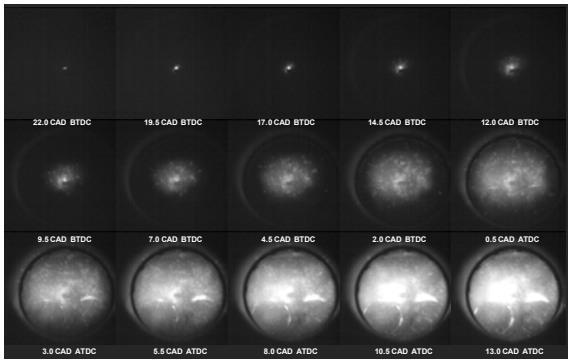

Fig. 11. Images detected in the first phase of the combustion process for 3-hole injector (average on 16 cycles).

[17]. An increase in the mean droplets size was observed in both injectors. At 70 CAD ATDC, the intake valves opened. The droplets moved to the combustion chamber and a decrease in their number together with an increase in the mean size were detected.

After reaching the combustion chamber, the fuel droplets stuck on the piston surfaces created fuel-rich zones that developed dynamically under the effect of the gas flow influencing the composition of the mixture and hence the combustion process. Analogous effects involved the fuel droplets stripped by the fuel film deposited onto the port wall or the back side of the inlet valve [6-8, 18-20]. To better understand the influences of these phenomena on the combustion process, cycle resolved imaging was performed.

Figs. 10-13 show the evolution of the combustion process from the start of spark to the reaching of the chamber walls in both the injectors. The images in Figs. 10 and 12 refer to a single engine cycle, while Figs. 11 and 13 show the average of the optical data acquired in 16 consecutive cycles. In this way it was possible to evaluate the overall behavior of the flame luminosity in each condition. The evidence of spark ignition was represented by a luminous arc near the spark plug and it occurred around 22 CAD BTDC. The flame kernel was well observable around 17 CAD BTDC, even if its luminosity was lower than the spark. Then flame kernel moved from the spark plug with a radial-like behavior until around TDC.

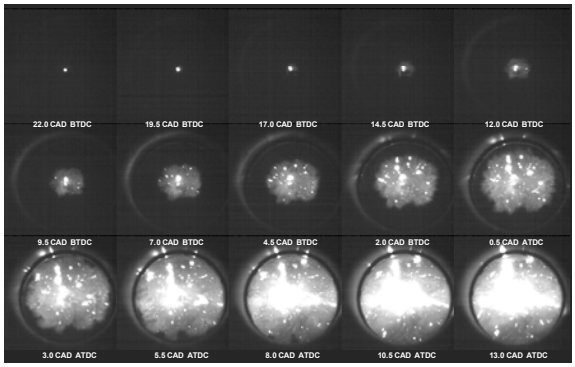

Fig. 12. Images detected in the first phase of the combustion process for 12-hole injector (single cycle).

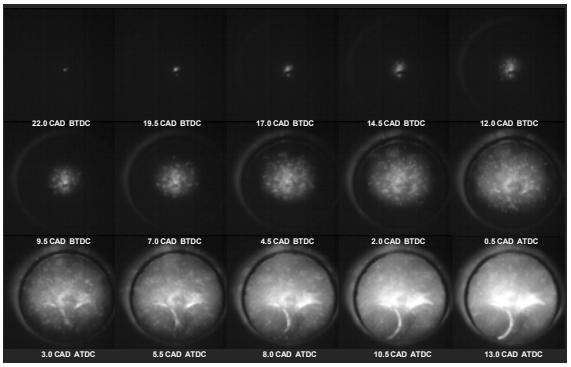

Fig. 13. Images detected in the first phase of the combustion process for 12-hole injector (average on 16 cycles).

Several bright spots were detected in the burned gas before the flame front reached the chamber walls. The bright spots were due to the fuel deposits on the optical window caused by the strip atomization of the fuel squeezing. The fuel deposits created fuel-rich zones with sub-millimeter size that ignited when reached by the normal flame front. When the injection occurred in the open valves state, this effect was enhanced by the partial carrying of the injected fuel droplets directly into the combustion chamber due to the gas flow. Part of these droplets was stuck on the cylinder walls and part was deposited on the piston surface. The bright spots are more evident for the single cycle, due to their random nature.

The presence of fuel deposits as squeezed film or impinged droplets had direct effect on flame radius evolution in terms of kernel cyclic variability and flame stability [21, 22]. When a flame propagates in the normal direction to an area with equivalence ratio gradient, each part of the front evolves in a field with varying fuel concentration. This induces variation of the propagation speed along the flame front and an increase in flame wrinkling.

Fig. 14 reports the trend of flame radius evaluated on 16 consecutive cycles for both injectors. It must be noted that around 4 CAD BTDC a change in flame radius evolution was detected. It was due to the flame front approaching the intake valve area. The higher fuel amount near the intake valves for the 3-hole injector induced more fuel-rich zones that slowed

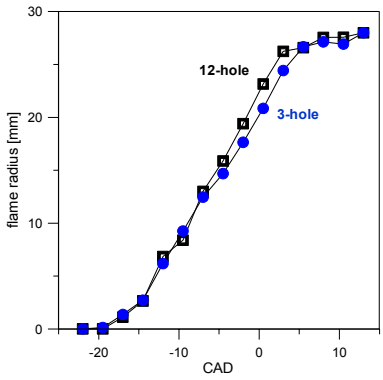

(a)

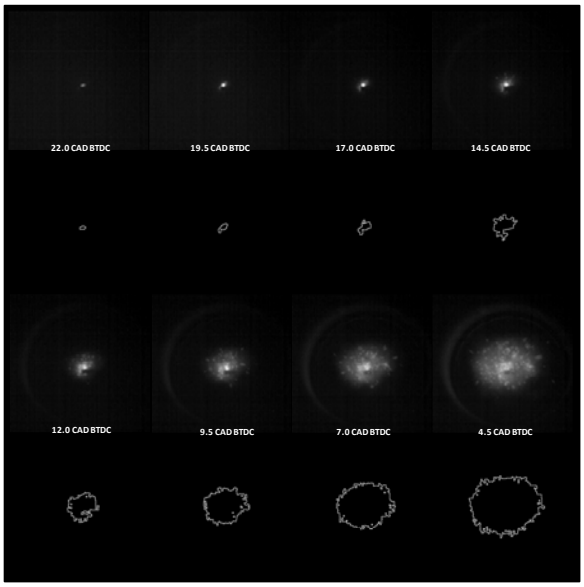

(b)

Fig. 14. (a) Flame radius evaluated by the averaged combustion process visualization; (b) comparison between the raw image and processed image for the 3-hole injector.

down the flame front. After the interaction with the intake valves, the flame occupied the whole optical field of view of the combustion chamber around 5 CAD ATDC.

Previous spectroscopic investigations associated the emission signals around 430 nm from spark ignition to 4 CAD ATDC to the CH radicals. These results supported the use of chemiluminescence to follow CH evolution in the combustion chamber. As known from the literature, CH radical is a flame front marker because it exists only in a narrow layer of the reaction zone taking part in the decomposition process of the fuel molecules in hydrocarbon flames [23]. Fig. 15 reports the CH spatial distributions for both injectors measured in the first phase of the combustion process. Around 12 CAD BTDC, CH distribution was strongly influenced by the spark plug position. At 7 CAD BTDC the radial-like outline of the reaction zone typical of the flame kernel was measured. From 2 CAD BTDC, the CH propagation was influenced by the lack of homogeneity in the mixture distribution caused by the fuel

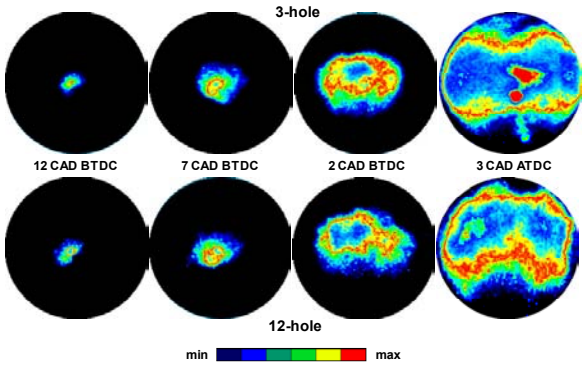

Fig. 15. CH radical evolution.

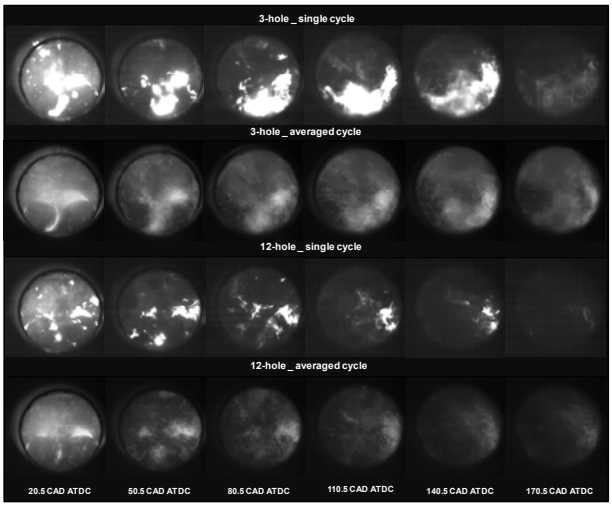

Fig. 16. Images detected in the late phase of the combustion process.

film deposition near the intake valves. Moreover, CH islands in the flame front were detected. They were caused by burning of the fuel deposits due to the stripping of squeezed film and/or to the impinged droplets, as observed in Figs. 9-12. These deposits strongly interfered with the local air-fuel ratio creating locally fuel rich zones even if the oxygen sensor measured a stoichiometric lambda value.

As shown in Figs. 9-12, around 10 CAD ATDC, the flame front interacted with the fuel deposits on the intake valves and diffusion-controlled flames with high luminosity were observed [6, 19]. As shown in Fig. 16, these flames persisted in the late combustion phase and their optical evidence could be detected until the exhaust valves opening. Formation of diffusive flames was possible since the oxygen was not completely consumed after the normal flame front propagation. In both conditions the time inception of the diffusion flames was equivalent and the highest flames intensity was observed near the intake valves. The diffusive flames were more intense in the 3-hole injector than 12-hole injector because of the different fuel amount deposited on the valves. For the 3-hole injector, the luminosity remained high until the exhaust valves opening. At this point the gas motion from the intake to the

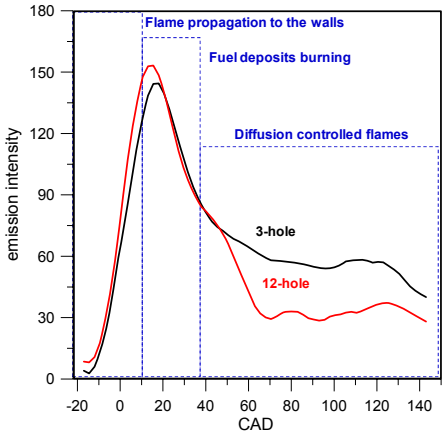

Fig. 17. Flame emission intensity evaluated by the averaged combustion process visualization.

exhaust valves determined the presence of diffusive flames also in the chamber center. In the 12-hole injector, the flames consumed almost completely the fuel, and their luminosity was negligible at the opening of exhaust valves.

A global approach to the combustion process can be obtained analyzing the integral luminous intensity averaged on 16 consecutives cycles as reported in Fig. 17. Different phases of the combustion process are outlined. The first started with the spark luminosity and concerned flame inception and propagation from the spark plug in the cylinder center to the cylinder walls. The better air fuel mixing induced by the 12-hole injector lightly increased the flame speed if compared to 3-hole injector as demonstrated by the higher luminosity rate. Around 12-15 CAD ATDC, the fresh mixture was almost totally burned and the luminosity increase was partially supported by the fuel deposits burning. This effect cannot be so clearly revealed though the heat release signal. At around 40-50 CAD ATDC, the well mixed fuel and air have been consumed, the further luminosity increase is caused by the diffusive flames that originate from the burning of fuel deposited on the intake valves and on the cylinder walls. The lower amount of fuel deposition for the 12-hole injector is featured by a lower luminosity in the late combustion phase with respect to the 3-hole injector. To better outline the injection modes effect on the combustion process, the cycle-to-cycle variation of the luminosity was measured in the whole combustion chamber in the late combustion phase (from 40 CAD ATDC to 140 CAD ATDC) and on the whole engine cycle. The results are shown in Fig. 18. Using the 12-hole injector a higher stability of the flame emission and of the combustion process was obtained.

Finally, the effect of the injectors on the exhaust emissions was measured. Fig. 19 reports variation in percentage of gas emission specific concentration measured at the exhaust for the 12-hole injector versus the 3-hole. It can be observed that the 12-hole injector induced a CO2, opacity and NOx decrease. An increase in HC and CO was also measured.

The reduction in opacity is related to the reduction in fuel

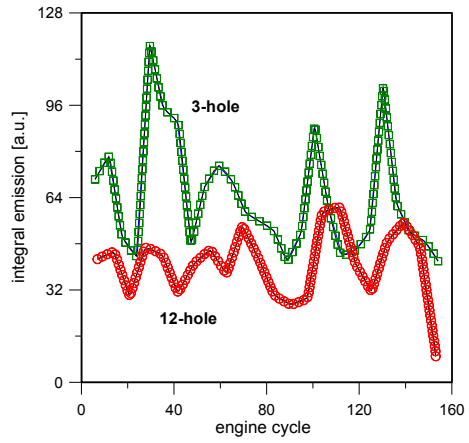

(a)

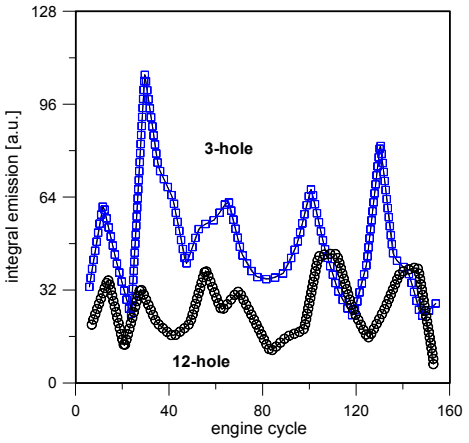

(b)

Fig. 18. Cycle-to-cycle evolution of the integral luminosity measured in the combustion chamber (a) in the late combustion phase (b) on the whole engine cycle.

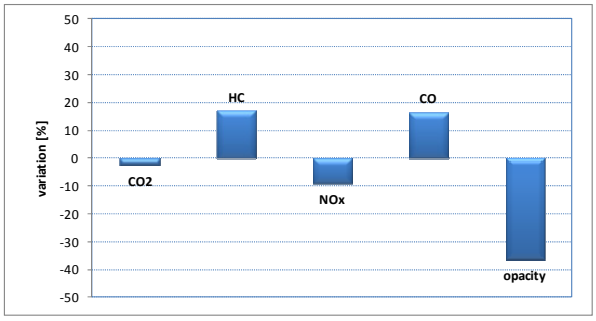

Fig. 19. Percentage variation of the exhaust emission of 12-hole injector versus 3-hole one.

deposits on the intake valves and piston surfaces. The lower amount of deposited fuel induced the formation of less intense diffusive flames that are sources of soot particles.

A review of the literature suggests that the most relevant mechanism for nitrogen oxide emissions from spark ignition engines [24] is the Zeldovich mechanism. It is generally referred to as thermal mechanism that is highly sensitive to temperature and oxygen concentration.

The different amount of NOx produced with the two injectors is probably caused by different temporal and spatial distribution of the air to fuel ratio in the two cases. In fact, as reported in the literature, changes in factors such as flame geometry and mixture properties influence the NOx formation. Early flame development is influenced by flow and mixture near the spark plug electrode. The turbulent flow can convect the flame, and differences in flame center motion influence later flame growth and wall interaction events. The varying flame geometry results in varying burn rates. Quenching phenomena can occur during the expansion stroke, and gas temperatures fall resulting in a partial burn and increased HC and CO emissions together with a NOx reduction.

4. Conclusions

The target of optimizing small engines for urban cars and two-wheel vehicles, scooters and motorcycles needs the detailed knowledge of thermo-fluid dynamic phenomena occurring during the fuel injection and the combustion process. Small-size SI engines generally operate at fairly high speed so that mixture preparation and devices that affect the quality of mixture are crucial for the engine performance. Nowadays the combustion process in SI engines can be improved further by enhancing the mixing process and changing the parameters that critically influence the combustion in a practical perspective.

In this work, the improvement of spray/mixture preparation and the following combustion behavior when applying 12-hole injector to a small engine for motorcycles was investigated. The effect of different injectors with 3 holes and 12 holes was studied comparing the results obtained in the intake manifold, in the combustion chamber and at the exhaust. Optical diagnostics were supported by post-detection image procedures and by in-cylinder and exhaust conventional measurements. All the measurements were realized in an optical accessible engine with the same geometrical parameters, head and injection system of a reference real engine.

The experimental results suggested that the multi-hole injector had a positive effect on the distribution of fuel droplets in the intake manifold: the distribution was more homogeneous than for 3 hole injector.

The 12-hole injector allowed reducing the wall wetting and fuel film deposits formation. The wall wetting interferes with the control of fuel delivery. In fact, over-fuelling in port fuel injected gasoline engines is required to compensate for wall wetting and the poor evaporation process especially under cold starting conditions.

The change of fuel injector from 3 holes to 12 holes induced a strong reduction in opacity value. The reduction in opacity is related to the reduction in fuel deposits on the intake valves and piston surfaces. The lower amount of deposited fuel induced the formation of less intense diffusive flames that are sources of soot particles.

The results obtained in this work suggest that the use of multi-hole injection systems can be a short-end and medium-cost solution for fuel consumption and pollutant emission.

Acknowledgment

The authors are grateful to Mr. Carlo Rossi and Mr. Bruno Sgammato for the assessment of the optical engine and for the support in the experimental activities.

References

[1] R. R. Maly, State of the art and future needs in S.I. engine combustion, *Symposium (International) on Combustion*, *Twenty-Fifth Symposium (International) on Combustion*, 25 (1) (1994) 111-124.

[2] M. C. Drake and D. C. Haworth, Advanced gasoline engine development using optical diagnostics and numerical modeling, *Proc. of the Combustion Institute*, 31 (1) (2007) 99-124.

[3] A. Stella, G. Guj, J. Kompenhans, H. Richard and M. Raffel, Three-component particle image velocimetry measurements in premixed flames, *Aerosp Sci Technol,* 5 (2001) 357-364.

[4] L. Withrow and G. M. Rassweiler, Studying engine combustion by physical methods a review, *J. Appl. Phys*. 9 (1938) 363-372.

[5] S. V. Sankar, K. E. Maher, D. M. Robart and W. D. Bachalo, Rapid characterization of fuel atomizers using an optical patternator, *J Eng Gas Turb Power*, 121 (1999) 409-414.

[6] S. N. Soid and Z. A. Zainal, Spray and combustion characterization for internal combustion engines using optical measuring techniques: A review- *Energy,* 36 (2011) 724-741.

[7] V. S. Costanzo and J. B. Heywood, Mixture preparation mechanisms in a port fuel injected engine, SAE Paper No. 2005-01-2080 (2005).

[8] M. Behnia and B. E. Milton, Fundamentals of fuel film formation and motion in SI engine induction systems*, Energy Conversion and Management,* 42 (15-17) (2001) 1751-1768.

[9] B. E. Milton, M. Behnia and D. M. Ellerman, Fuel deposition and re-atomisation from fuel/air flows through engine inlet valves, *Int. Journal of Heat and Fluid Flow*, 22 (3) (2001) 350-357.

[10] J. B. Heywood, *Internal Combustion Engine Fundamentals,* New York: McGraw-Hill (1988).

[11] J. B. Blaisot and J. Yon, Droplet size and morphology characterization for dense sprays by image processing: application to the Diesel spray, *Experiments in Fluids*, 39 (2005) 977-994.

[12] L. M. R. Brás, E. F. Gomes, M. M. M. Ribeiro and M. M. L. Guimarães, Drop distribution determination in a liquid-liquid dispersion by image processing, *International Journal of Chemical Engineering* (2009) Article ID 746439, 6 pages.

[13] J. Hacohen, M. R. Belmont, R. W. F. Thurley, J. C. Thomas, E. L. Morris and D. J. Buckingham, Experimental and theoretical analysis of flame development and misfire phenomena in a spark-ignition engine, SAE paper n. 920412 (1992) .

[14] S. S. Merola, B. M. Vaglieco, G. Formisano, G. Lucignano and G. Mastrangelo, Flame diagnostics in the combustion chamber of boosted PFI SI engine, SAE paper n. 2007-24-0003 (2007).

[15] O. Mörsch and P. Sorsche, (DaimlerChrysler AG) Investigation of alternative methods to determine particulate mass emissions, http://www.oica.net/htdocs.

[16] Y-P. Wang, G. B. Wilkinson and J. A. Drallmeier, Parametric study on the fuel film breakup of a cold start PFI engine, *Experiments in Fluids,* 37 (3) (2004) 385-398.

[17] S. M. Begg, M. P. Hindle, T. Cowell and M. R. Heikal, Low intake valve lift in a port fuel-injected engine*, Energy,* 34 (2009) 2042-2050.

[18] M. R. Gold, C. Arcoumanis, J. H. Whitelaw, J. Gaade and S. Wallace, Mixture preparation strategies in an optical four-valve port-injected gasoline engine, *Int. Journal of Engine Research*, 1 (1) (2000) 41-56.

[19] T. Nogi, Y. Ohyama, T. Yamauchi and H. Kuroiwa, Mixture formation of fuel injection systems in gasoline engines, SAE Paper n. 880558 (1988).

[20] R. Meyer and J. B. Heywood, Liquid fuel transport mechanisms into the cylinder of a firing port-injected SI engine during start up, SAE Paper No. 970865 (1997).

[21] Y. Bianco, W. Cheng and J. Heywood, The effects of initial flame kernel conditions on flame development in si engines, SAE paper n. 912402 (1992).

[22] P. Witze, M. Hall and M. Bennet, Cycle-resolved measurements of flame kernel growth and motion correlated with combustion duration, SAE paper n. 900023 (1990).

[23] C. M. Vagelopoulos and J. H. Frank, An experimental and numerical study on the adequacy of CH as a flame marker in premixed methane flames, *Proceedings of the Combustion Institute* 30 (2005) 241-249.

[24] R. R. Raine, C. R. Stone and J. Gould, Modeling of nitric oxide formation in spark ignition engines with a multizone burned gas*, Combustion and Flame*, 102 (3) (1995) 241-255.

Simona Silvia Merola received from the University of Naples in Italy her "Summa cum Laude" Magister Degree in Physics in 1995 and Ph.D in Chemical Engineering in 2000. Since 2001 she has been a Researcher in Istituto Motori of the Italian National Research Council, specializing in the application of optical diagnostics to the combustion process investigation. Her research work focuses on the experimental analysis of the thermo fluid-dynamic phenomena that occur in-cylinder and at the exhaust of the internal combustion engines. Since 1996, she has been involved with and has the direct responsibility for experimental activities in several national and international research projects.

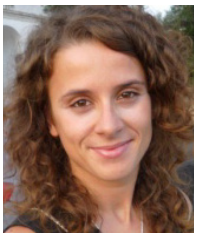

Cinzia Tornatore received from the University of Naples in Italy her "Summa cum Laude" Magister Degree in Chemical Engineering in 2004 and Ph.D in Chemical Engineering in 2007. Her education activities were focused on the optical diagnostics of nanoparticles at internal combustion engines exhaust. From 2007 to 2011 she worked as Associate Researcher at Istituto Motori of "Italian National Research Council". Since 2011 she is full position Researcher and she is involved in research projects on the optical characterization of combustion process in internal combustion engines.

Paolo Sementa received his Magister Degree in Mechanical Engineering from the University of Naples in Italy in 2006. Afterwards he has been Associate Researcher at Istituto Motori of "Italian National Research Council". In 2011 he became full position researcher. He works on the assessment and optimization of the transparent internal combustion engines. He takes part in research projects on fuel injection and combustion process investigation in I.C. engines.